Silva Fennica vol. 58 no. 3 article id 23061
Category: research article
https://doi.org/10.14214/sf.23061
SILVA FENNICA
http://www.silvafennica.fi
ISSN-L 0037-5330 | ISSN 2242-4075 (Online)
The Finnish Society of Forest Science

CC BY SA

Special issue: Climate resilient and sustainable forest management

Noora Tienaho[1], Ninni Saarinen[1], Tuomas Yrttimaa[1], Ville Kankare[1] and Mikko Vastaranta[1]

Quantifying fire-induced changes in ground vegetation using bitemporal terrestrial laser scanning

Tienaho N., Saarinen N., Yrttimaa T., Kankare V., Vastaranta M. (2024). Quantifying fire-induced changes in ground vegetation using bitemporal terrestrial laser scanning. Silva Fennica vol. 58 no. 3 article id 23061. 20 p. https://doi.org/10.14214/sf.23061

Highlights

- Bitemporal terrestrial laser scanning provided a means for identifying surface areas exposed to fire by utilizing a surface differencing method developed in this study.
- The developed method allowed for the quantification of fire-induced volumetric changes in ground vegetation at high resolution, facilitating the assessment of the impact of surface fires on forest ecosystems.

Abstract

Forest fires pose a significant threat to forest carbon storage and sinks, yet they also play a crucial role in the natural dynamics of boreal forests. Accurate quantification of biomass changes resulting from forest fires is essential for damage assessment and controlled burning evaluation. This study utilized terrestrial laser scanning (TLS) to quantify changes in ground vegetation resulting from low-intensity surface fires. TLS data were collected before and after controlled burnings at eight one-hectare test sites in Scots pine (*Pinus sylvestris* L.) dominated boreal forests in Finland. A surface differencing-based method was developed to identify areas exposed to fire. Validation, based on visual interpretation of 1 × 1 m surface patches (n = 320), showed a recall, precision, and F1-score of 0.9 for the accuracy of identifying burned surfaces. The developed method allowed the assessment of the magnitude of fire-induced vegetation changes within the test sites. The proportions of burned 1 × 1 m areas within the test sites varied between 51–96%. Total volumetric change in ground vegetation was on average –1200 m^3 ha^{-1}, with burning reducing the vegetation volume by 1700 m^3 ha^{-1} and vegetation growth increasing it by 500 m^3 ha^{-1}. Substantial variations in the volumetric changes within and between the test sites were detected, highlighting the complex dynamics of surface fires, and emphasizing the importance of having observations from multiple sites. This study demonstrates that bitemporal TLS measurements provide a robust means for characterizing fire-induced changes, facilitating the assessment of the impact of surface fires on forest ecosystems.

Keywords biomass; boreal forest; controlled burning; forest fires; LiDAR; surface differencing; surface fires
Addresses [1]School of Forest Sciences, University of Eastern Finland, P.O. Box 111, 80101 Joensuu, Finland
E-mail noora.tienaho@uef.fi
Received 18 October 2023 **Revised** 16 April 2024 **Accepted** 19 April 2024

1 Introduction

Fires are among the most significant disturbances reducing forest biomass (Pugh et al. 2019), and with climate change, both the frequency and intensity of forest fires are expected to increase (Flannigan et al. 2005; Keywood et al. 2013; Jolly et al. 2015). Fires also contribute to global warming by releasing carbon dioxide (CO_2) during combustion and by destroying vegetation, which would otherwise serve as a CO_2 sink (Szpakowski and Jensen 2019). Yet, forest fires play a vital role in the natural dynamics of boreal forests. Fires create mosaic patterns of different-aged forest stands, incorporating varying amounts of charred and decaying wood, which provide habitats for a diverse range of species (Parviainen 1996; Ryan 2002; Jonsson et al. 2005). Particularly in Fennoscandian boreal forests, the occurrence of wildfires has decreased significantly (Lindberg et al. 2018), necessitating controlled burning to preserve forest biodiversity. Consequently, quantifying the fire-induced biomass changes in the boreal forests is important for evaluating both the extent of wildfire damage and the effectiveness of controlled burning as a management strategy for sustaining and enhancing biodiversity.

Forest fires can be categorized as crown, surface, and ground fires based on the type of fuelbed (Lindberg et al. 2011; Greene and Michaletz 2015). Crown fires refer to the flaming combustion of the forest canopy, surface fires primarily burn the ground vegetation, and ground fires involve the smoldering combustion of the organic topsoil and roots near the soil (Greene and Michaletz 2015; Pérez-Izquierdo et al. 2020). In Fennoscandian boreal forests, non-stand replacing ground and surface fires are more common than high-intensity crown fires (Päätalo 1998; Rogers et al. 2015). Ground vegetation burning in surface fires consists of shrub, herbal, and moss layers (Marozas et al. 2007; Buriánek et al. 2013). Additionally, surface fires might consume understory trees and the fuel load accumulated on the forest floor, including trees that have been thinned and left on the ground.

Direct measurement of biomass requires destructive sampling of plant materials, involving the collection, drying, and weighing of plant samples from the targeted area (Houghton 2008; Olsoy et al. 2014). However, conducting destructive sampling at a landscape scale is both expensive and impractical (Olsoy et al. 2014), and it prevents repeated monitoring necessary for change detection (Greaves et al. 2015). Among indirect measurement methods, allometric equations are commonly utilized (Houghton 2008), yet their applicability is often limited to trees and may not extend to ground vegetation or other biomass components on the forest floor.

Laser scanning offers a non-destructive approach for estimating the amount of aboveground biomass consumed by forest fires. This technique enables direct acquisition of three-dimensional (3D) coordinates of objects. Laser scanning operates by emitting laser pulses towards a target and detecting the reflected energy. By considering the constant velocity of light, the time taken for a pulse to return to the sensor can be converted into a distance measurement. When coupled with a global navigation satellite system (GNSS) and an inertial measurement unit (IMU), the precise position and orientation of the sensor can be determined, enabling the conversion of these distance measurements into a 3D characterization of the environment. Each returning echo is assigned a 3D coordinate within a designated coordinate system, resulting in a comprehensive 3D point cloud. These point clouds can then be utilized to quantify the dimensions of vegetative structures and fire-induced volumetric changes. Laser scanning encompasses both aerial and terrestrial applications. Airborne laser scanning (ALS) is particularly suitable for assessing variations in the height and density of the upper canopy since it operates from above the canopy. Conversely, terrestrial laser scanning (TLS) offers more detailed information about the lower forest strata by scanning from below the canopy. Measurements taken above the canopy often yield sparser laser returns and larger laser footprints, which could potentially lead to underestimations of ground vegetation height or even misclassification as ground (Riaño et al. 2007; Vierling et al. 2013; Greaves et al. 2015).

TLS is known for providing highly accurate 3D data at the millimeter scale (Liang et al. 2016), making it suitable for quantifying small-scale changes in forest vegetation. While the feasibility of TLS to estimate aboveground biomass and volume of individual trees has been extensively studied (Lin et al. 2010; Seidel et al. 2011; Yao et al. 2011; Moskal and Zheng 2012), the characterization of ground vegetation with TLS has received relatively less attention. Previous studies have focused on estimating sagebrush biomass (Olsoy et al. 2014), biomass of shrub species (Greaves et al. 2015), and fuelbed volume (Loudermilk et al. 2009; Rowell et al. 2020). These studies have employed techniques such as 3D convex hull modeling, voxel counting, and surface differencing to estimate the biomass or volume of ground vegetation. The experiments have shown high agreement between the TLS-based estimates and destructive sampling ($R^2 = 0.9$) (Olsoy et al. 2014; Greaves et al. 2015), indicating that TLS is well-suited for estimating quantities of ground vegetation. This suggests that TLS could be a feasible means for monitoring changes in ground vegetation caused by surface fires.

To accurately quantify fire-induced biomass changes, bitemporal measurements are required, but their implementation is often challenging due to the unpredictable nature of wildfires. Nonetheless, controlled burnings provide opportunities for planned experiments. In forestry, controlled or prescribed burning refers to the deliberate use of fire for silvicultural or nature management purposes. This practice serves various functions worldwide, including reducing fuel load to prevent future forest fires, controlling diseases or insect pests, and restoring ecosystems. In Fennoscandian boreal forests, controlled burnings have traditionally been employed after final felling to enhance reforestation (Karjalainen 1994; Lemberg and Puttonen 2002). However, in recent times, they are primarily conducted for restorative purposes as the natural occurrence of forest fires has decreased (Lindberg et al. 2020). In Finland, controlled burnings specifically target the vegetation on the forest floor, and the fire is not allowed to spread into the canopies. Thus, they resemble the behavior of surface fires.

This study aims to utilize bitemporal TLS measurements to quantify changes in ground vegetation resulting from low-intensity surface fires in pine-dominated boreal forests. TLS has not been widely employed in the boreal region for detecting fire-induced changes in ground vegetation. Consequently, the surface area exposed to fire, the volume of burned ground vegetation, and the variability of these across different sites remain poorly understood. Given that the majority of forest fires in Fennoscandian boreal forests are low-intensity surface fires, developing robust means for measuring and understanding the effects of these fires is important.

The first research question of this study investigates whether fire-induced changes in ground vegetation can be identified using TLS measurements conducted pre- and post-fire. The related hypothesis is that an analysis of changes in detailed surface models characterizing the height of ground vegetation can reveal surface patches exposed to fire, indicating burned vegetation. Due to the time lag between the TLS acquisitions and the characteristics of surface fires, the observed changes will consist of decreased vegetation height due to fire and increased vegetation height due to growth. To further examine these changes, the test sites are divided into 1 × 1 m cells, classified as ‘burned’ and ‘unburned’ based on the analysis of changes in detailed surface models. The performance of the developed method is evaluated against a set of validation samples acquired through visual interpretation.

Consequently, the second research question is whether the magnitude of fire-induced vegetation changes can be assessed using the developed surface differencing-based method. The hypothesis is that an analysis of volumetric changes in ground vegetation, coupled with the obtained information regarding the geospatial locations of surface patches exposed to fire, allows for the volumetric quantification of burned vegetation. To provide insights into mapping of fire-induced changes in ground vegetation and estimating the magnitude of burned vegetation, the approach is tested on eight test sites with varying pre-fire characteristics.

2 Material and methods

2.1 Experimental design and data acquisition

The experimental design included eight test sites located in national parks or protected areas across southern Finland (Fig. 1). These sites underwent controlled burnings by Metsähallitus during the summers of 2021 and 2022, with the aim of ecological restoration. All test sites are situated in the central or southern boreal zone and are dominated by Scots pine. The forest types include dry heath, sub-xeric heath, and mesic heath (classified according to Cajander's (1926) categorization as *Calluna* type, *Vaccinium* type, and *Myrtillus* type) (Table 1). The ground vegetation in pine-dominated forests in Fennoscandia typically consists of feather mosses (*Pleurozium schreberi* (Willd. ex Brid.) Mitt., *Hylocomium splendens* (Hedw.) Schimp.) and dwarf shrubs (*Vaccinium myrtillus* L., *Vaccinium vitis-idaea* L.) (Palviainen et al. 2005). After a fire event, early successional species such as *Agrostis capillaris* L., *Chamerion angustifolium* (L.) Holub, and *Melampyrum pratense* L. usually invade the areas (Marozas et al. 2007). With the exception of test sites 'Pyhä-Häkki', 'Ruunaa', and 'Salamajärvi', all the other test sites had been thinned prior to the controlled burnings, resulting in logging residues on the forest floor. Approximately one-hectare sample plots were established in

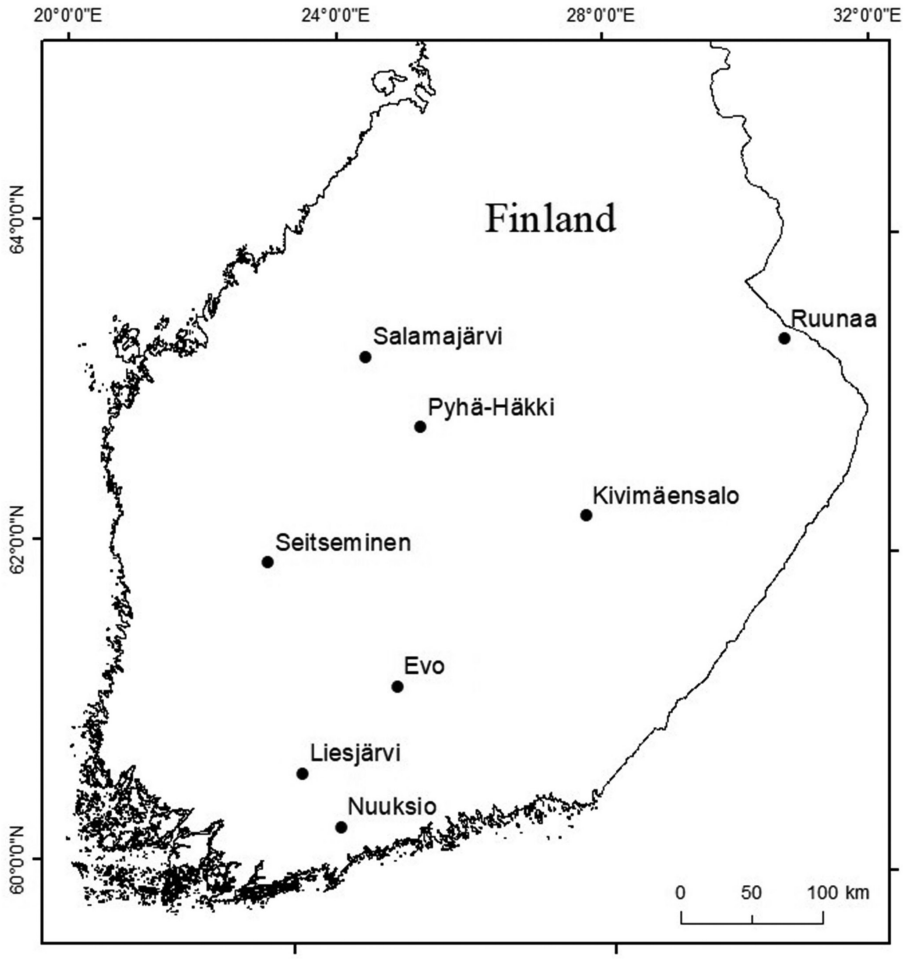

Fig. 1. Eight controlled burning sites in southern Finland marked with black dots. The test sites 'Kivimäensalo', 'Liesjärvi', 'Pyhä-Häkki', 'Nuuksio', and 'Seitseminen' were burned in 2021, whereas 'Evo', 'Ruunaa', and 'Salamajärvi' in 2022. All the test sites are located within national parks or protected areas.

Table 1. Coordinates of the center of each test site, forest types, and dates of controlled burnings and pre- and post-fire terrestrial laser scanning (TLS) measurements. The test sites are located in southern Finland.

Site	Coordinates (N, E)	Forest type	Pre-fire TLS	Burning	Post-fire TLS
Kivimäensalo	62°18.419', 27°41.495'	mesic heath	10 Jun 2021	6 Jul 2021	9 Sep 2021
Liesjärvi	60°39.043', 24°1.070'	sub-xeric heath	16 Jun 2021	17 Jun 2021	5 Sep 2021
Pyhä-Häkki	62°51.358', 25°25.417'	sub-xeric heath	13 Jun 2021	30 Jun 2021	7 Sep 2021
Nuuksio	60°19.484', 24°32.349'	sub-xeric heath	6 Jun 2021	7 Jun 2021	30 Jun 2021
Seitseminen	61°58.080', 23°24.735'	sub-xeric heath	20 Jun 2021	1 Jul 2021	6 Sep 2021
Evo	61°13.342', 25°11.761'	mesic heath	3 Jun 2022	15 Aug 2022	18 Aug 2022
Ruunaa	63°22.814', 30°30.132'	sub-xeric heath	9 Jun 2022	30 Jun 2022	3 Jul 2022
Salamajärvi	63°17.267', 24°37.976'	dry heath	13 Jul 2022	16 Aug 2022	13 Sep 2022

each of the sites, and TLS measurements were conducted both before (i.e., pre-fire) and after the fire (i.e., post-fire). The time interval between pre- and post-fire TLS measurements ranged from one to three months (Table 1). Visual representations of one of the controlled burning sites before and after the fire are provided in Fig. 2.

The TLS measurements were performed using a Riegl VZ-400i time-of-flight laser scanner (RIEGL Laser Measurement Systems, Horn, Austria), which operates at a wavelength of 1550 nm. This scanner can capture multiple returns per emitted laser pulse and provides a 100° vertical and a 360° horizontal field of view. To ensure point cloud coverage of each test site, a multi-scan approach was adopted. This involved acquiring multiple individual scans with a regular 10 × 10 m grid for the scanner locations, resulting in an overall setup consisting of approximately 120 scans per test site. The scanner operated at a pulse repetition rate of 600 kHz, capturing up to eight returns for each emitted laser pulse. The beam divergence was 0.35 mrad at $1/e^2$. The applied 'Panorama 40' scan pattern had an angular resolution of 0.04° and a point spacing of 3.5 mm at a 10 m distance.

Fig. 2. The test site 'Evo' two months before (left) and a few days after (right) the controlled burning.

The scans were co-registered into a merged point cloud for each site, and points with extreme reflectance values (< –25 dB and > 5 dB) were subsequently removed. This process followed a standard procedure using the RiSCAN PRO software provided by the scanner manufacturer. The scanner was equipped with integrated orientation and positioning sensors, including an IMU and a GNSS receiver, allowing for the acquisition and registration of multi-scan point clouds without the need for artificial reference targets. The coordinates of the test site corners were measured using the Trimble Geo 7X (Trimble Inc., Westminster, USA) equipped with real-time extended (RTX) GNSS positioning. The merged point clouds were then clipped using polygons created from these corner coordinates.

2.2 Point cloud processing

The TLS point clouds were processed using LAStools software (version 211218) (Isenburg 2021). Controlled burnings conducted between TLS data acquisitions prevented the use of external reflective targets with known locations for georeferencing the pre- and post-fire point clouds. Instead, the scanner's GNSS receiver, providing approximately 1–2 m positioning accuracy under the forest canopy, was utilized. Due to variation in the GNSS positioning accuracy between the pre- and post-fire TLS measurements, the acquired point clouds exhibited slight misalignment. As achieving precise positioning of the pre- and post-fire point clouds was critical for change detection, a rigid 3D transformation was applied to ensure proper point cloud alignment. Consequently, xyz-coordinates of tie points common to both pre- and post-fire measurements were manually extracted. These tie points (8 per site) represented objects reliably distinguishable within the point clouds, such as branch origins, as shown in Fig. 3.

The extracted tie point coordinates were then used to compute xyz-translation and xy-rotation along the z-axis for the pre-fire point clouds, aligning them with the post-fire point clouds. The xyz-translation was computed as an arithmetic mean of the coordinate differences between the tie points. For xy-rotation, the angle and center of rotation were determined for each test site by examining the intersections of bisectors of line segments connecting two misaligned tie-point pairs (Ryan 2019). The implemented alignments were visually inspected and further refined to ensure that the pre- and post-fire point clouds were as closely aligned as possible.

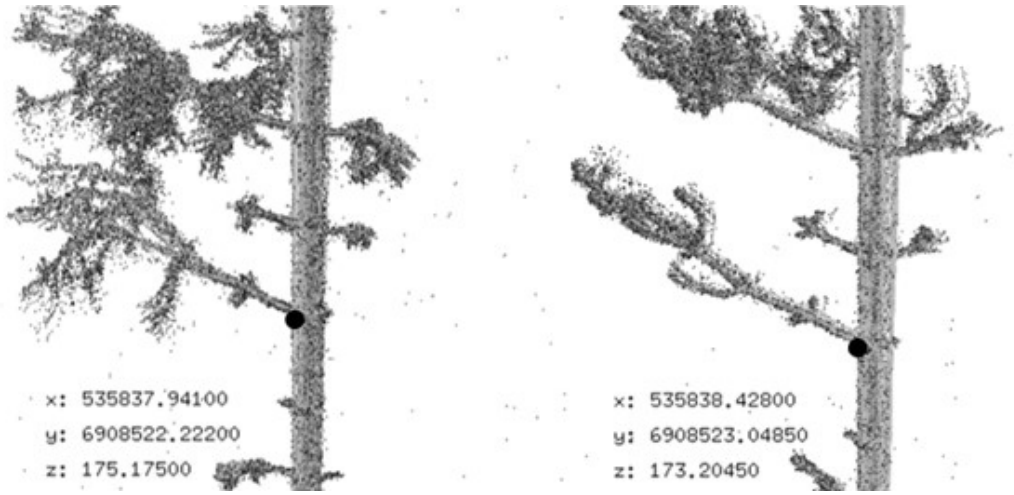

Fig. 3. Pre-fire point clouds (left) were aligned with post-fire point clouds (right) using a 3D transformation derived from common tie points, e.g., the large black dots in the figure. The tie points were manually extracted from the point clouds.

Coordinates of the point clouds were rescaled to an accuracy of 1 mm to reduce the number of decimals and the size of the processed point cloud files. To remove noisy points caused by erroneous measurements, the lasnoise tool was employed. Points with less than six neighboring points within a radius of 2 cm were removed. Subsequently, the denoised point clouds were downsampled and voxelized into a 5 mm 3D grid to achieve uniform point density and further decrease the size of the point clouds while preserving structural details.

Points were classified into ground and non-ground points using the lasground_new tool, following the procedure presented in Ritter et al. (2017). Digital elevation models (DEMs) were subsequently generated using the las2dem tool, which temporarily triangulates points into a triangulated irregular network (TIN) before rasterizing it into a DEM via linear interpolation. DEMs were produced at a 1 m resolution. The generation was based on the post-fire TLS measurements, assuming that the ground surface would be more visible after the fire. These DEMs were utilized to normalize both the pre- and post-fire point clouds. As the controlled burnings only affected ground vegetation, points located more than 2 meters above the ground surface were omitted from further analysis.

2.3 Stand characteristics

Stand characteristics for each test site were derived from the pre-fire TLS point clouds using methods presented in Yrttimaa et al. (2019, 2020) and available in Yrttimaa (2021). These methods involved automatic tree detection, separation of stem points from non-stem points, and computation of single tree attributes that were used for estimating the stand characteristics of each test site. The analysis was performed using MATLAB (version R2023a). The stand characteristics included the number of stems, basal area, basal area weighted mean diameter at breast height, basal area weighted mean height, stem volume, and canopy cover. These characteristics provided a general description of the test sites. Stand age assessment was obtained from Metsähallitus. Elevation data was derived from the post-fire DEMs, and the mean elevation within the test sites ranged from 100 to 190 m. The stand characteristics and mean elevation are presented in Table 2.

Table 2. Stand characteristics and mean elevation of controlled burning sites. N = number of stems, G = basal area, D_g = basal area weighted mean diameter at breast height, H_g = basal area weighted mean height, Vol = stem volume, CC = canopy cover. The test sites are located in southern Finland.

Site	Area (ha)	N (ha^{-1})	G ($m^2\ ha^{-1}$)	D_g (cm)	H_g (m)	Vol ($m^3\ ha^{-1}$)	CC (%)	Stand age (~y)	Elevation (m)
Kivimäensalo	1.2	732	17.1	18.7	16.9	140	54	60	164
Liesjärvi	1.0	527	12.7	19.2	16.1	93	42	60	140
Pyhä-Häkki	1.0	1 147	31.4	21.7	18.3	261	79	70	176
Nuuksio	1.1	369	21.2	31.0	20.6	205	55	150	100
Seitseminen	1.0	687	25.3	24.3	21.6	260	55	50	184
Evo	1.2	751	23.7	26.3	18.6	210	68	60	171
Ruunaa	0.9	948	28.5	21.5	19.6	274	76	120	152
Salamajärvi	1.0	919	30.7	23.0	19.6	272	65	70	190

2.4 Identifying surface patches exposed to fire

The bitemporal TLS point clouds were utilized to identify areas exposed to fire. This identification was based on an assumption that a decrease in vegetation height indicates burned vegetation, while an increase or no change in vegetation height indicates unburned vegetation. For this assessment, pre- and post-fire vegetation surface models were generated on a two-dimensional (2D) grid at a 0.1 m resolution, with each cell representing the vegetation height. The vegetation height was determined based on the 99th height percentile, representing the height below which 99% of the points within the cell could be found. The 99th height percentile was preferred over maximum height due to previous studies suggesting that 90–99th height percentiles correlate better with field measurements of ground vegetation height, as the presence of extreme points can introduce noise and affect the accuracy of the maximum height measurement (Friedli et al. 2016; Malambo et al. 2018).

Although the TLS scan setup involved many scans per site, in forest conditions, it is typical that not all structural details can be reconstructed due to occlusion caused, for example, by vegetation or topography. Therefore, surface models were interpolated to fill in the missing values for cells with no point returns. Interpolation was performed for both the pre- and post-fire surface models using the mean value of the nearest 9 × 9 cells. When generating the surface models, all the 3D points below 2 m were considered, including points originating from tree stems. Changes in ground vegetation height were estimated using surface differencing, which involved subtracting the pre-fire surface models from post-fire surface models. Points originating from tree stems were subtracted in this differencing, since the stems remained stationary. As a result of surface differencing, negative values indicated a decrease in ground vegetation height, while positive values indicated an increase.

The detailed surface models of changes in ground vegetation height were then aggregated into 1 × 1 m cells to provide a more concise view of the changes and to reduce noise caused by fine-scale variability. These 1 × 1 m cells were classified as either ‘burned’ or ‘unburned’ based on the proportion of burned 0.1 × 0.1 m cells they contained. If more than half of the smaller cells showed a negative change in vegetation height, the 1 × 1 m cell was classified as ‘burned’. Otherwise, the cell was classified as ‘unburned’. This classification method ensured that the presence of a single large growth of ground vegetation (e.g., tall grass) within an otherwise burned cell would not identify the cell as unburned. The proportion of burned and unburned areas were calculated from these classified 1 × 1 m cells and visualized with maps.

2.5 Assessment of classification method

The performance of the classification method for ‘burned’ and ‘unburned’ areas was assessed by randomly sampling 20 ‘burned’ and 20 ‘unburned’ 1 × 1 m cells from each test site and visually interpreting the point clouds. Equal allocation was employed due to the lower number of ‘unburned’ cells, and because distinguishing between burned and unburned areas was crucial. Different colored pre- and post-fire point clouds were overlaid, and a cell was considered ‘burned’ if the majority of points in the pre-fire point cloud were higher than those in the post-fire point cloud. Subsequently, recall, precision, and F1-score were utilized to measure the classification accuracy. Recall quantifies the ratio of true positives identified by the classification method to the total number of true positives, as determined by visual interpretation. Precision, on the other hand, quantifies the ratio of true positives to the total number of positives (both correctly and incorrectly identified). F1-score integrates both precision and recall, providing a comprehensive assessment of the classification method’s performance within a single metric. In this study, ‘true positive’ refers to a 1 × 1 m cell classified as ‘burned’ based on both TLS measurements and visual inspection. ‘False positive’ indicates a cell that is not burned according to visual inspection. Similarly, ‘true negative’ is clas-

sified as 'unburned' by both methods, while 'false negative' indicates a cell that is not identified as 'unburned' according to visual inspection. The accuracy measures were calculated with equations:

$$Recall = \frac{TP}{TP + FN} \quad (1)$$

$$Precision = \frac{TP}{TP + FP} \quad (2)$$

$$F1 = 2 \times \frac{Precision \times Recall}{Precision + \mathrm{Re}\,call} \quad (3)$$

where TP = true positive, FN = false negative, and FP = false positive. These metrics were calculated for each test site.

2.6 Quantifying volumetric changes in ground vegetation

The pre- and post-fire vegetation surface models, at a 0.1 m resolution, were utilized to estimate the ground vegetation volume at both time points by multiplying the height of each cell by its area. Subsequently, the total pre- and post-fire ground vegetation volume estimates were derived by summing these values. The total change was estimated by subtracting the pre-fire total ground vegetation volume from the post-fire volume. The total ground vegetation volume changes included both the decrease caused by fire and the increase caused by growth, and these changes were investigated separately at a 0.1 m resolution. The variation of the volume changes within the test sites was examined in the 1 × 1 m cells classified as 'burned' and 'unburned', and the distributions of these changes were visualized using Tukey's boxplots.

3 Results

3.1 Identifying burned and unburned areas

Out of the total number of 320 cells (1 × 1 m), 284 were correctly identified (i.e., classified as 'burned' or 'unburned') using the developed method, resulting in a mean recall of 0.90. The remaining 36 cells were falsely identified, leading to a mean precision of 0.89. Consequently, the cells were classified with an accuracy of 0.88 when measured by the F1-score. The identification accuracy varied between the test sites, with recall ranging between 0.77–0.95, precision ranging between 0.65–1.00, and F1-score between 0.74–0.98 (Table 3).

Table 3. Recall, precision, and F1-score quantifying the performance of the classification method for identifying 'burned' and 'unburned' areas for each controlled burning site.

Site	Recall	Precision	F1-score
Kivimäensalo	0.95	1.00	0.98
Liesjärvi	0.77	1.00	0.87
Pyhä-Häkki	0.95	0.95	0.95
Nuuksio	0.94	0.80	0.86
Seitseminen	0.80	1.00	0.89
Evo	0.87	0.65	0.74
Ruunaa	0.95	0.95	0.95
Salamajärvi	0.94	0.75	0.83
Mean	0.90	0.89	0.88

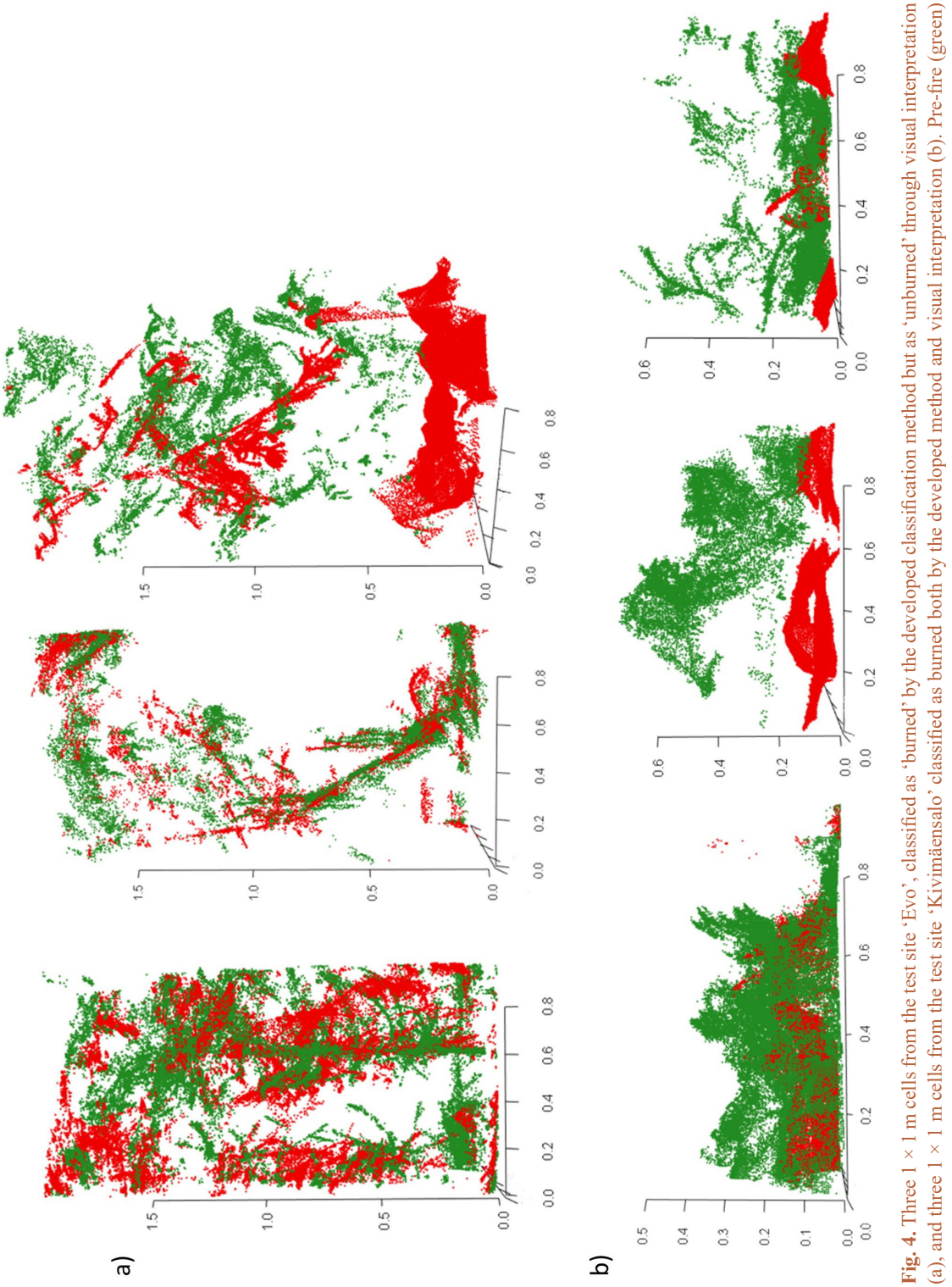

Fig. 4. Three 1 × 1 m cells from the test site 'Evo', classified as 'burned' by the developed classification method but as 'unburned' through visual interpretation (a), and three 1 × 1 m cells from the test site 'Kivimäensalo' classified as burned both by the developed method and visual interpretation (b). Pre-fire (green) and post-fire (red) point clouds are overlaid.

Table 4. Proportions of 1 × 1 m cells classified as 'burned' and 'unburned' for each controlled burning site.

Site	Proportion of 1 × 1 m cells	
	'Burned'	'Unburned'
Kivimäensalo	95%	5%
Liesjärvi	95%	5%
Pyhä-Häkki	92%	8%
Nuuksio	83%	17%
Seitseminen	94%	6%
Evo	51%	49%
Ruunaa	96%	4%
Salamajärvi	71%	29%

In the test site 'Evo', both precision and consequently F1-score were lower compared to other test sites, indicating that with the developed method, cells were classified as 'burned' even though visual inspection of point clouds determined them to be 'unburned'. Fig. 4 depicts three such cells, and for comparison, three true positive cells from the test site 'Kivimäensalo'.

3.2 Quantifying changes in ground vegetation

Using the developed method for identifying surface patches exposed to fire, it was possible to quantify the total burned area as well as estimate the magnitude of volumetric changes in ground vegetation, caused either by fire or vegetation growth. The proportion of 1 × 1 m cells classified as 'burned' varied between the controlled burning sites being the lowest in the test site 'Evo' (51%) and the highest in the test site 'Ruunaa' (96%) (Table 4). Correspondingly, the proportion of 'unburned' cells ranged from 4% to 49%. Maps of surface areas exposed to fire are presented in Fig. 5.

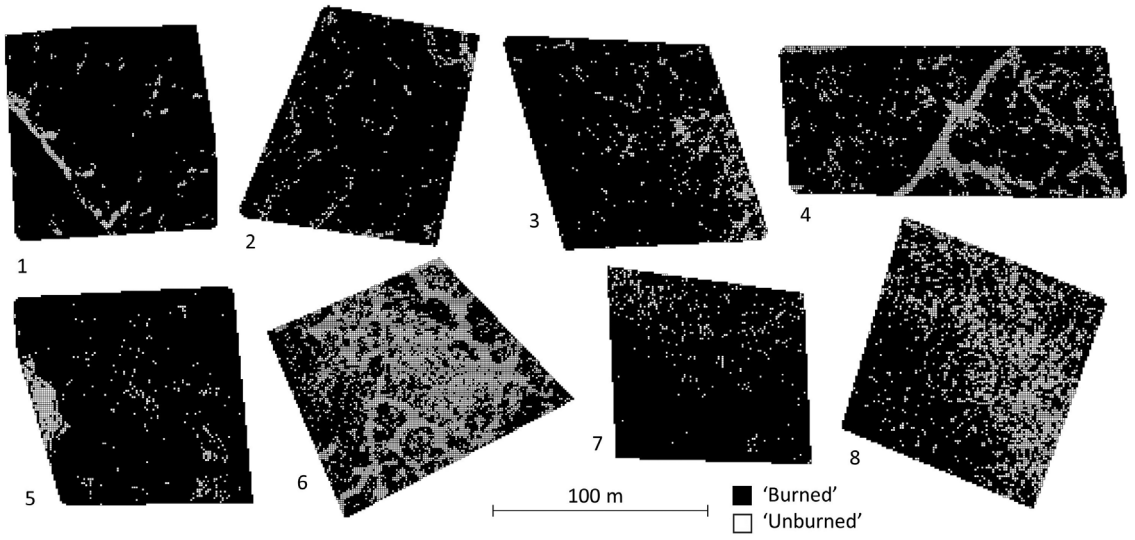

Fig. 5. Spatial distribution of 1 × 1 m cells classified as 'burned' and 'unburned' for each controlled burning site. Test sites are oriented in a north-south direction. 1 = Kivimäensalo, 2 = Liesjärvi, 3 = Pyhä-Häkki, 4 = Nuuksio, 5 = Seitseminen, 6 = Evo, 7 = Ruunaa, 8 = Salamajärvi.

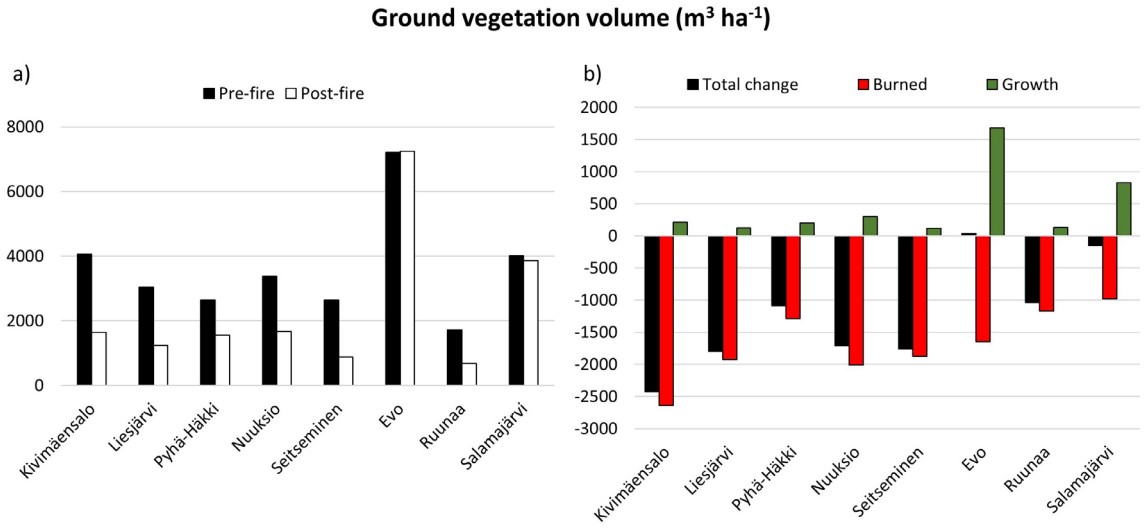

Fig. 6. Ground vegetation volumes (including tree stems below 2 m) before and after controlled burnings (a), and total changes (black) with burned (red) and growth (green) volumes (b) at a resolution of 0.1 m. Negative values indicate a decrease and positive values an increase in ground vegetation volume.

Substantial variations in ground vegetation volume changes within and between controlled burnings were detected. The test site 'Evo' had the largest pre- and post-fire ground vegetation volumes (including tree stems below 2 m), 7206 and 7242 m^3 ha^{-1}, respectively, while 'Ruunaa' had the smallest, 1718 and 682 m^3 ha^{-1} respectively (Fig. 6a). The total volume change in ground vegetation ranged from –2422 to 33 m^3 ha^{-1}, including both a decrease due to burning and an increase due to vegetation growth (Fig. 6b). Ground vegetation volume decreased in all other test sites except in 'Evo', where the total amount of ground vegetation increased between the TLS measurements. The largest burned ground vegetation volume was observed in 'Kivimäensalo' (–2637 m^3 ha^{-1}), while the smallest burned volume occurred in 'Salamajärvi' (–981 m^3 ha^{-1}) (Fig. 6b). Conversely, the largest vegetation growth was observed in 'Evo' (1679 m^3 ha^{-1}), and the lowest in 'Seitseminen' (115 m^3 ha^{-1}).

For the 1 × 1 m cells classified as 'burned', the median volume change of burned ground vegetation was the largest in Kivimäensalo (–0.23 m^3) and the lowest in 'Salamajärvi' (–0.04 m^3) (Fig. 7a). The highest standard deviation of volume change among the 'burned' cells was observed in 'Evo' (0.22 m^3), and the lowest in 'Ruunaa' (0.10 m^3). For the cells classified as 'unburned', the median volume change was the lowest in 'Liesjärvi' (–0.01 m^3) and the largest in 'Evo' (0.13 m^3) (Fig. 7b) The highest standard deviation among 'unburned' cells was observed in 'Evo' (0.23 m^3), and the lowest in 'Liesjärvi (0.07 m^3).

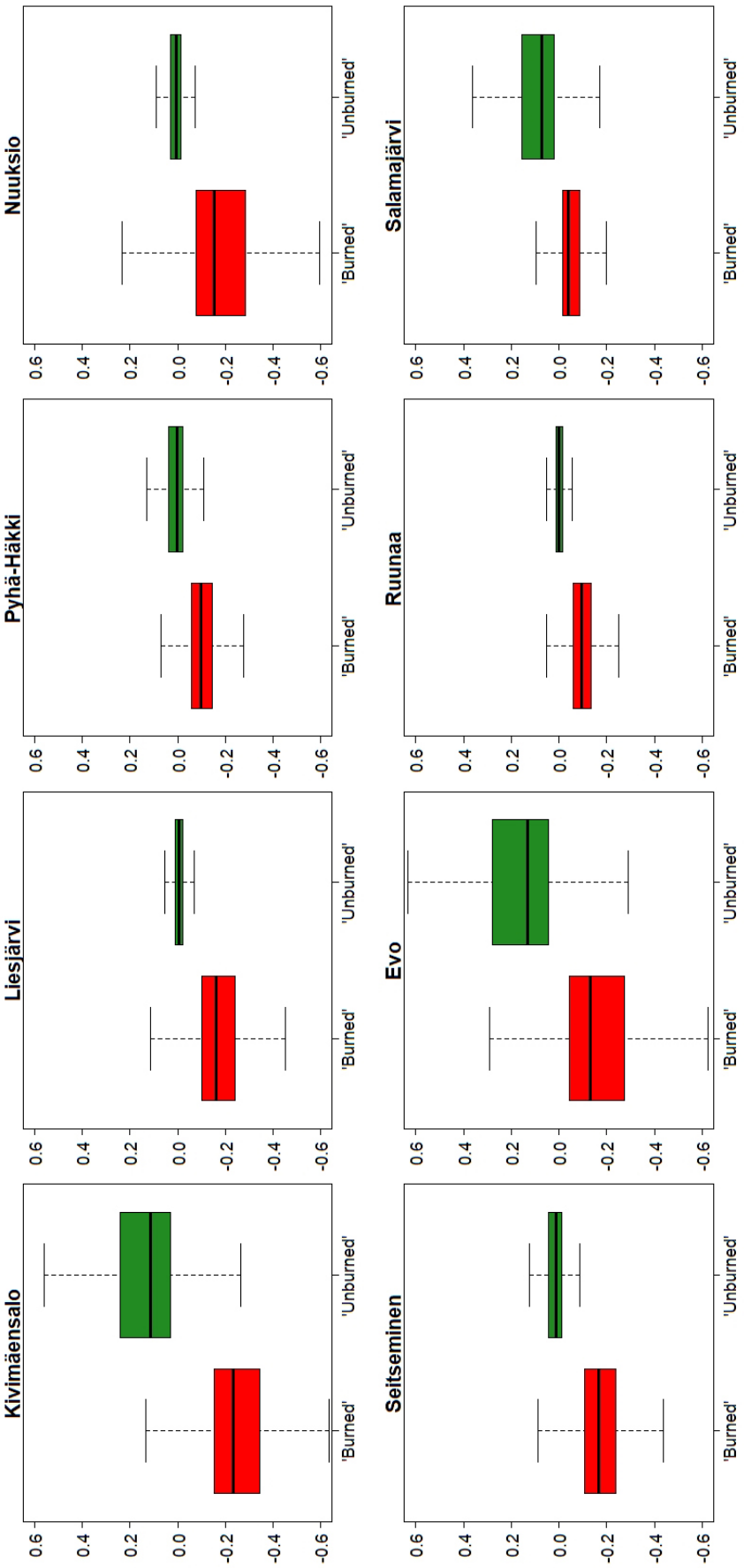

Fig. 7. Variation in ground vegetation volume changes in 1 × 1 m cells classified as 'burned' and 'unburned' in the controlled burning sites. The line in the box center represents the median value; the box represents the middle 50% of the cell values; 25% of the values fall below the lower quartile (bottom of the box), and 75% fall below the upper quartile (top of the box); whiskers represent minimum and maximum cell values. Outliers (i.e., 0.35% of the observations both above and below the whiskers) are not shown in the figure to enhance the display of data distribution and variability.

4 Discussion

4.1 Identifying burned and unburned areas

The aim of this study was to utilize bitemporal TLS measurements to quantify fire-induced changes in ground vegetation. More specifically, the objectives were to identify surface areas exposed to fire, estimate the magnitude of changes in ground vegetation volume, and examine the variation in fire-induced changes within and between eight test sites.

The first research question focused on identifying burned and unburned areas using pre- and post-fire TLS measurements. This identification was executed by comparing detailed surface models that captured the height of ground vegetation before and after the fire. The developed classification method for 1 × 1 m cells performed well, achieving an overall accuracy ranging between 0.74–0.98 when assessed by the F1-score (Table 3). The study site 'Evo' yielded the lowest F1-score, likely due to denser ground vegetation compared to other test sites. As depicted in Fig. 4, dense spruce undergrowth, combined with minor non-fire-related changes above the ground surface, may result in misclassification of the cell as 'burned'. Nevertheless, the overall results provided strong evidence supporting the hypothesis that the presented method enables the identification of areas exposed to fire.

In previous studies it has noted that controlled burning results in a mosaic of burned and unburned areas (Penman et al. 2007; Perkiö et al. 2012), indicating that the vegetation on the forest floor is not completely consumed by the fire. For example, Gupta et al. (2015) observed that in the controlled burning of sclerophyll eucalypt forests, approximately 60–70% of the study area was affected by the fire. The uneven effect of fire is ecologically desirable as it leads to the creation of diverse habitats. In this study, the proportions of burned areas within the test sites varied between 51–96% (Table 4). Maps created from the burned areas will help to visualize the overall fire pattern and, for instance, assess the realization of the controlled burning.

4.2 Quantifying volumetric changes in ground vegetation

The second research question explored the capacity of TLS to quantify fire-induced volumetric changes in ground vegetation using the developed surface differencing-based method. The method was applied across different test sites to assess the magnitude and variation in burned vegetation. The total volumetric changes ranged from –2422 to 33 m^3 ha^{-1} across the controlled burning sites, including both decreases and increases in vegetation volume. The fire-induced negative volumetric changes ranged from –2637 to –981 m^3 ha^{-1}, while the growth-induced positive volumetric changes varied between 115 and 1679 m^3 ha^{-1}. Internal volume variability within the test sites was examined in 1 × 1 m cells classified as 'burned' and 'unburned', with their mean standard deviations being 0.15 m^3 and 0.12 m^3, respectively.

Variations in volume changes can partly be attributed to site characteristics, including factors such as tree number and size, which affect light and nutrient availability due to tree competition, soil moisture, and litter accumulation (Xiong and Nilsson 1999; Ludwig et al. 2004). These factors influence both the quantity and quality of ground vegetation and fuel load. For example, in sites 'Kivimäensalo' and 'Evo', which had a more nutrient-rich forest type compared to others (Table 1), the internal volume variability both in 'burned' and 'unburned' cells was the highest. Additionally, in 'Kivimäensalo', the overall change in ground vegetation volume was the largest. Differences in pre-fire ground vegetation volume can also explain the variations in changes.

In 'Salamajärvi', ground vegetation volume decreased only by 154 m^3 ha^{-1}, and in 'Evo', it increased. This could be influenced by the longer time interval between the first TLS measure-

ment and the burning compared to other test sites (Table 1). Burnings in 'Evo' and 'Salamajärvi' occurred in August instead of the optimal period from mid-May to the end of June (Laurila and Vierula 2020), further explaining these anomalies.

The site 'Evo' stands out from the other controlled burning sites in several aspects. Firstly, it had the largest 'unburned' area, and it was the only site featuring an increase in the ground vegetation volume (Fig. 6). 'Evo' exhibited the largest pre- and post-fire volumes in ground vegetation (Fig. 6), and the standard deviations of the ground vegetation volume changes were the highest (0.22 m^3 in 'burned' and 0.23 m^3 in 'unburned' 1 × 1 m cells). These findings indicate that in 'Evo', the impact of fire was more inconsistent. Additionally, the substantial increase of the ground vegetation volume suggests favorable growth conditions and indeed, 'Evo' was more nutrient-rich in terms of forest type. However, these distinctions are not evident in the stand characteristics outlined in Table 2.

The unique fire behavior observed in 'Evo' highlights the significant variation among the test sites. Therefore, solely focusing on one area could lead to erroneous conclusions and predictions. Conversely, examining changes across multiple controlled burning sites enabled a more comprehensive understanding of variability and patterns in fire behavior. Detailed investigations at this scale enhanced the reliability and generalizability of these findings. However, it is worth mentioning that the primary objective of this study was to develop a method for detecting and quantifying changes with TLS measurements rather than explaining their causes.

4.3 Challenges and prospects for future research

Surface differencing, the method employed in this study to quantify ground vegetation changes, assumes that the space below the observed vegetation surface is fully occupied by vegetation or fuel load. This may have led to an overestimation of the volume in cells where the highest point was reflected from a loose branch, for example. Ground vegetation volume could also be estimated using the convex hull method or voxel counting (Loudermilk et al. 2009; Olsoy et al. 2014; Graeves et al. 2015). Surface differencing was selected as the method because, for instance, Zhao et al. (2021) demonstrated that it exhibited the strongest correlation with field-measured biomass when estimating shrub volume in grassland, outperforming other methods. Comparing the results obtained by different methods with boreal forest data could be beneficial, but the most crucial aspect is carefully validating the selected method as done in this study. Fire-induced changes in ground vegetation could be investigated not only through height variation but also by examining vegetation density characteristics or changes in ground surface elevation. This presents opportunities for further research.

From the ground vegetation volume estimated in this study, it is possible to proceed to the estimation of the amount of biomass, but this relationship heavily relies on the density, distribution, and characteristics of the burned vegetation. Directly evaluating biomass would have necessitated the collection, drying, and weighing of ground vegetation samples, which exceeded the scope of this study. For future studies, samples obtained through destructive methods would be necessary to accurately estimate biomass changes. When combined with destructive sampling, TLS-estimated biomass changes can be converted into CO_2 equivalents, facilitating the assessment of the climatic impacts of low-intensity fires. Moreover, by monitoring vegetation recovery and tree mortality post-fire, it becomes feasible to evaluate the longer-term effects of surface fires on the forest ecosystem.

In this study, the pre-measurements were conducted on average 20 days before the controlled burnings, and the post-measurements on average 40 days after. Consequently, areas not affected by the fire were able to continue growing for an average of 70 days (Table 1). Therefore, if the ground vegetation had grown between the pre-fire measurements and the controlled burning, the estimated burned volume may have been underestimated, while the increased volume

may have been overestimated. While the ground vegetation volume in burned areas likely had remained relatively stable until the post-fire measurements, the overestimation of biomass may still have increased in unburned areas due to vegetation growth after the fire. Given the influence of growth, it is important to schedule the bitemporal TLS campaign as close to the burning dates as possible in the future. However, this can be challenging due to the strong dependency of controlled burning on weather conditions and if the burnings are conducted by an external party, as in this study.

The behavior of the fire and subsequent volume changes are also strongly influenced by the implementation of controlled burning. Factors such as ignition, control, extinguishing, and the timing of the burn all contribute to the dynamics of a fire (Lemberg and Puttonen 2002; Laurila and Vierula 2020). To prevent the fire from spreading beyond the intended areas, abundant watering is often employed before, during, and after controlled burning. Additionally, the areas designated for burning are usually demarcated by firebreaks or fire lines. Firebreaks, typically 5–25 m wide, involve the removal of trees and combustible materials, while fire lines are narrower strips with exposed mineral soil (Lindberg et al. 2011; Perkiö et al. 2012; Laurila and Vierula 2020). These firebreaks and lines are intentionally kept unburned either through watering or exposing mineral soil. In this study, assessing the impact of these factors was not feasible as it would have required measurements, such as continuous monitoring of the fire during its occurrence, which were beyond the scope. This presents an avenue for future research.

5 Conclusion

This study utilized bitemporal TLS measurements to quantify changes in ground vegetation resulting from low-intensity surface fires in Scots pine-dominated boreal forests. A surface differencing-based classification method was developed and validated to identify surface areas exposed to fire, achieving a recall, precision, and F1-score of 0.9. Ground vegetation volume changes were estimated across eight controlled burning sites in southern Finland. The variation in volume changes within and across the sites highlighted the complex dynamics of surface fires. Based on the insights gained from this study, TLS measurements acquired pre- and post-fire provide a robust means for characterizing fire-induced changes in vegetation, thereby facilitating the assessment of the impact of surface fires on forest ecosystems.

Declaration of openness of research materials, data, and code

Data are available on request from the corresponding author.

Authors' contributions

Conceptualization (N.T.; N.S.; T.Y.; V.K.; M.V.), data curation (N.T.) data analysis (N.T.; N.S.; T.Y.), writing – original draft preparation (N.T.), visualization (N.T.), writing – review and editing, (N.T.; N.S.; T.Y.; V.K.; M.V), project administration (M.V.). All authors have read and agreed to the published version of the manuscript.

Funding

This research was funded by the Academy of Finland and European Union (NextGenerationEU) through projects "Understanding wood density variation within and between trees using multi-spectral point cloud technologies and X-ray microdensitometry" (Density4Trees, 331711) and "Capturing structural and functional diversity of trees and tree communities for supporting sustainable use of forests" (Diversity4Forests, 348643), and by Flagship "Forest-human-machine interplay – building resilience, redefining value networks and enabling meaningful experiences" (UNITE, 357906).

References

Buriánek V, Novotný R, Hellebrandová K, Šrámek V (2013) Ground vegetation as an important factor in the biodiversity of forest ecosystems and its evaluation in regard to nitrogen deposition. J For Sci 59: 238–252. https://doi.org/10.17221/16/2013-JFS.

Cajander AK (1926) The theory of forest types. Acta For Fenn 29, article id 7193. https://doi.org/10.14214/aff.7193.

Flannigan MD, Amiro BD, Logan KA, Stocks BJ, Wotton BM (2005) Forest fires and climate change in the 21st century. Mitig Adapt Strateg Glob Chang 11: 847–859. https://doi.org/10.1007/s11027-005-9020-7.

Friedli M, Kirchgessner N, Grieder C, Liebisch F, Mannale M, Walter A (2016) Terrestrial 3D laser scanning to track the increase in canopy height of both monocot and dicot crop species under field conditions. Plant Methods 12, article id 9. https://doi.org/10.1186/s13007-016-0109-7.

Greaves HE, Vierling LA, Eitel JUH, Boelman NT, Magney TS, Prager CM, Griffin KL (2015) Estimating aboveground biomass and leaf area of low-stature Arctic shrubs with terrestrial LiDAR. Remote Sens Environ 164: 26–35. https://doi.org/10.1016/j.rse.2015.02.023.

Greene DF, Michaletz ST (2015) The role of fire in forest ecosystems. In: Peh KSH, Corlett RT, Bergeron Y (eds) Routledge handbook of forest ecology. Routledge, London, pp 114–126.

Gupta V, Reinke KJ, Jones SD, Wallace L, Holden L (2015) Assessing metrics for estimating fire induced change in the forest understorey structure using terrestrial laser scanning. Remote Sens 7: 8180–8201. https://doi.org/10.3390/rs70608180.

Houghton RA (2008) Biomass. In: Jørgensen SE, Fath BD (eds) Encyclopedia of ecology. Elsevier, Amsterdam, pp 448–453. https://doi.org/10.1016/B978-008045405-4.00462-6.

Isenburg M (2021) LAStools – efficient LiDAR processing software (version 211218, academic). http://rapidlasso.com/LAStools. Accessed 19 October 2023.

Jolly WM, Cochrane MA, Freeborn PH, Holden ZA, Brown TJ, Williamson GJ, Bowman DMJS (2015) Climate-induced variations in global wildfire danger from 1979 to 2013. Nat Commun 6, article id 7537. https://doi.org/10.1038/ncomms8537.

Jonsson BG, Kruys N, Ranius T (2005) Ecology of species living on dead wood – lessons for dead wood management. Silva Fenn 39: 289–309. https://doi.org/10.14214/sf.390.

Karjalainen J (1994) Tuli pohjoisissa havumetsissä ja metsänhoidollinen kulotus. [Fire in northern coniferous forests and restorative burning]. Metsähallitus, Vantaa.

Keywood M, Kanakidou M, Stohl A, Dentener F, Grassi G, Meyer CP, Torseth K, Edwards D, Thompson AM, Lohmann U, Burrows J (2013) Fire in the air: biomass burning impacts in a changing climate. Crit Rev Env Sci Tec 43: 40–83. https://doi.org/10.1080/10643389.2011.604248.

Laurila J, Vierula J (2020) Kulotusopas. [Controlled burning guide]. Suomen metsäkeskus, Sei-

näjoki.
Lemberg K, Puttonen P (2002) Kulottajan käsikirja. [Handbook for controlled burning]. Metsälehti Kustannus, Helsinki.
Liang X, Kankare V, Hyyppä J, Wang Y, Kukko A, Haggrén H, Yu X, Kaartinen H, Jaakkola A, Guan F, Holopainen M, Vastaranta M (2016) Terrestrial laser scanning in forest inventories. ISPRS J Photogramm Remote Sens 115: 63–77. https://doi.org/10.1016/j.isprsjprs.2016.01.006.
Lin Y, Jaakkola A, Hyyppä J, Kaartinen H (2010) From TLS to VLS: biomass estimation at individual tree level. Remote Sens 2: 1864–1879. https://doi.org/10.3390/rs2081864.
Lindberg H, Heikkilä TV, Vanha-Majamaa I (2011) Suomen metsien paloainekset – kohti parempaa tulen hallintaa. [Finnish forest fuels – towards improved fire management]. Metsäntutkimuslaitos, Vantaa. http://urn.fi/URN:ISBN:978-951-40-2294-4.
Lindberg H, Saaristo L, Nieminen A (2018) Tuli takaisin metsiin – kulotuksiin kannustamisen perusteet, tavoitteet ja tukeminen. [Returning fire to forests – basics, objectives, and support for controlled burning]. Tapio, Helsinki.
Lindberg H, Punttila P, Vanha-Majamaa I (2020) The challenge of combining variable retention and prescribed burning in Finland. Ecol Process 9, article id 4. https://doi.org/10.1186/s13717-019-0207-3.
Loudermilk EL, Hiers JK, O'Brien JJ, Mitchell RJ, Singhania A, Fernandez JC, Slatton KC (2009) Ground-based LIDAR: a novel approach to quantify fine-scale fuelbed characteristics. Int J Wildland Fire 18: 676–685. https://doi.org/10.1071/WF07138.
Ludwig F, de Kroon H, Berendse F, Prins HHT (2004) The influence of savanna trees on nutrient, water and light availability and the understorey vegetation. Plant Ecol 170: 93–105. https://doi.org/10.1023/B:VEGE.0000019023.29636.92.
Malambo L, Popescu SC, Murray SC, Putman E, Pugh NA, Horne DW, Richardson G, Sheridan R, Rooney WL, Avant R, Vidrine M, McCutchen B, Baltensperger D, Bishop M (2018) Multitemporal field-based plant height estimation using 3D point clouds generated from small unmanned aerial systems high-resolution imagery. Int J Appl Earth Obs Geoinf 64: 31–42. https://doi.org/10.1016/j.jag.2017.08.014.
Marozas V, Racinskas J, Bartkevicius E (2007) Dynamics of ground vegetation after surface fires in hemiboreal *Pinus sylvestris* forests. For Ecol Manag 250: 47–55. https://doi.org/10.1016/j.foreco.2007.03.008.
MATLAB (2023). Version 9.14.0.2137306 (R2023a). The MathWorks Inc, Natick, Massachusetts, United States.
Moskal LM, Zheng G (2012) Retrieving forest inventory variables with terrestrial laser scanning (TLS) in urban heterogeneous forest. Remote Sens 4: 1–20. https://doi.org/10.3390/rs4010001.
Olsoy PJ, Glenn NF, Clark PE, Derryberry DR (2014) Aboveground total and green biomass of dryland shrub derived from terrestrial laser scanning. ISPRS J Photogramm Remote Sens 88: 166–173. https://doi.org/10.1016/j.isprsjprs.2013.12.006.
Päätalo M-L (1998) Factors influencing occurrence and impacts of fires in northern European forests. Silva Fenn 32: 185–202. https://doi.org/10.14214/sf.695.
Palviainen M, Finér L, Mannerkoski H, Piirainen S, Starr M (2005) Responses of ground vegetation species to clear-cutting in a boreal forest: aboveground biomass and nutrient contents during the first 7 years. Ecol Res 20: 652–660. https://doi.org/10.1007/s11284-005-0078-1.
Parviainen J (1996) Impact of fire on Finnish forests in the past and today. Silva Fenn 30: 353–359. https://doi.org/10.14214/sf.a9246.
Penman TD, Kavanagh RP, Binns DL, Melick DR (2007) Patchiness of prescribed burns in dry sclerophyll eucalypt forests in South-eastern Australia. For Ecol Manag 252: 24–32. https://doi.org/10.1016/j.foreco.2007.06.004.

Pérez-Izquierdo L, Clemmensen KE, Strengbom J, Granath G, Wardle DA, Nilsson M-C, Lindahl BD (2020) Crown-fire severity is more important than ground-fire severity in determining soil fungal community development in the boreal forest. J Ecol 109: 504–518. https://doi.org/10.1111/1365-2745.13529.

Perkiö R, Puustonen M, Similä M (2012) Controlled burning to emulate natural forest fires. In: Similä M, Junninen K (eds) Ecological restoration and management in boreal forests – best practices from Finland. Metsähallitus, Vantaa.

Pugh TAM, Arneth A, Kautz M, Poulter B, Smith B (2019) Important role of forest disturbances in the global biomass turnover and carbon sinks. Nat Geosci 12: 730–735. https://doi.org/10.1038/s41561-019-0427-2.

Riaño D, Chuvieco E, Ustin SL, Salas J, Rodríguez-Pérez JR, Ribeiro LM, Viegas DX, Moreno JM, Fernández H (2007) Estimation of shrub height for fuel-type mapping combining airborne LiDAR and simultaneous color infrared ortho imaging. Int J Wildland Fire 16: 341–348. https://doi.org/10.1071/WF06003.

Ritter T, Schwarz M, Tockner A, Leisch F, Nothdurft A (2017) Automatic mapping of forest stands based on three-dimensional point clouds derived from terrestrial laser-scanning. Forests 8, article id 265. https://doi.org/10.3390/f8080265.

Rogers BM, Soja AJ, Goulden ML, Randerson JT (2015) Influence of tree species on continental differences in boreal fires and climate feedbacks. Nat Geosci 8: 228–234. https://doi.org/10.1038/ngeo2352.

Rowell E, Loudermilk EL, Hawley C, Pokswinski S, Seielstad C, Queen L, O'Brien JJ, Hudak AT, Goodrick S, Hiers JK (2020) Coupling terrestrial laser scanning with 3D fuel biomass sampling for advancing wildland fuels characterization. For Ecol Manag 462, article id 117945. https://doi.org/10.1016/j.foreco.2020.117945.

Ryan KC (2002) Dynamic interactions between forest structure and fire behavior in boreal ecosystems. Silva Fenn 36: 13–39. https://doi.org/10.14214/sf.548.

Ryan M (2019) Geometry essentials for dummies. John Wiley & Sons, Hoboken.

Seidel D, Beyer F, Hertel D, Fleck S, Leuschner C (2011) 3D-laser scanning: a non-destructive method for studying above- ground biomass and growth of juvenile trees. Agric For Meteorol 151: 1305–1311. https://doi.org/10.1016/j.agrformet.2011.05.013.

Szpakowski DM, Jensen JLR (2019) A review of the applications of remote sensing in fire ecology. Remote Sens 11, article id 2638. https://doi.org/10.3390/rs11222638.

Vierling LA, Xu Y, Eitel JUH, Oldow JS (2013) Shrub characterization using terrestrial laser scanning and implications for airborne LiDAR assessment. Can J Remote Sens 38: 709–722. https://doi.org/10.5588/m12-057.

Xiong S, Nilsson C (1999) The effects of plant litter on vegetation: a meta-analysis. J Ecol 87: 984–994. https://doi.org/10.1046/j.1365-2745.1999.00414.x.

Yao T, Yang X, Zhao F, Wang Z, Zhang Q, Jupp D, Lovell J, Culvenor D, Newnham G, Ni-Meister W, Schaaf C, Woodcock C, Wang J, Li X, Strahler A (2011) Measuring forest structure and biomass in New England forest stands using Echidna ground-based lidar. Remote Sens Environ 115: 2965–2974. https://doi.org/10.1016/j.rse.2010.03.019.

Yrttimaa T (2021) Automatic point cloud processing tools to characterize trees (PointCloud-Tools: v1.0.1). (v1.0.1). Zenodo. https://doi.org/10.5281/zenodo.5779288.

Yrttimaa T, Saarinen N, Kankare V, Liang X, Hyyppä J, Holopainen M, Vastaranta M (2019) Investigating the feasibility of multi-scan terrestrial laser scanning to characterize tree communities in southern boreal forests. Remote Sens 11, article id 1423. https://doi.org/10.3390/rs11121423.

Yrttimaa T, Saarinen N, Kankare V, Hynynen J, Huuskonen S, Holopainen M, Hyyppä J, Vastaranta M (2020) Performance of terrestrial laser scanning to characterize managed Scots pine (*Pinus*

sylvestris L.) stands is dependent on forest structural variation. ISPRS J Photogramm Remote Sens 168: 277–287. https://doi.org/10.1016/j.isprsjprs.2020.08.017.

Zhao Y, Liu X, Wang Y, Zheng Z, Zheng S, Zhao D, Bai Y (2021) UAV-based individual shrub aboveground biomass estimation calibrated against terrestrial LiDAR in a shrub-encroached grassland. Int J Appl Earth Obs Geoinf 101, article id 102358. https://doi.org/10.1016/j.jag.2021.102358.

Total of 49 references.